Non-Data-Aided Frequency-Offset and Channel Estimation in OFDM and Related Block Transmissions*

Xiaoli Ma[1], *Georgios B. Giannakis*[1] and *Sergio Barbarossa*[2]

[1] Dept. of ECE, Univ. of Minnesota; 200 Union Str. SE, Minneapolis, MN 55455, USA
[2] Infocom Dept., Univ. of Rome "La Sapienza", Via Eudossiana 18, 00184 Rome, ITALY

Abstract— **The many advantages responsible for the widespread application of OFDM are primarily limited by its sensitivity to carrier frequency offsets. Most of the literature dealing with this problem focuses on data-aided frequency offset estimation only. In this contribution, several non-data-aided frequency-offset and channel estimation schemes are developed for OFDM transmissions over frequency-selective channels. Timing offset is also accounted for because it is incorporated as a pure delay in the unknown channel. The resulting blind estimation methods include subspace based deterministic or statistical algorithms. Simulations illustrate performance tradeoffs of these schemes.**

I. Introduction

Orthogonal Frequency Division Multiplexing (OFDM) enables high data rate transmissions over frequency-selective channels at a relatively low complexity, and has been chosen as the transmission method for the European Digital Audio- and Video-Broadcasting (DAB and DVB) standards, as well as for the wireless local area networking standards (IEEE802.11a and HIPERLAN/2). Relying on multicarrier (MC) modulation, OFDM is robust against frequency selective fading and narrowband interference. With convolutional coding across subcarriers, OFDM also enables low-complexity Viterbi decoding. OFDM systems however, are more sensitive to carrier frequency offset (CFO) than single carrier modulations. CFO destroys subcarrier orthogonality and the resulting intercarrier interference degrades Bit Error Rate (BER) performance severely [11]. Thus, estimation and compensation of CFO are performance-critical tasks before demodulation at the receiver.

The available CFO estimators for OFDM can be classified in two categories: data-aided [10, 13], and non-data-aided [3, 7, 9]. Two training blocks (OFDM symbols) and oversampling are used in [13] (see also [10] for an extension using only one training block, and [9] for a blind method). Although [9] offers the maximum likelihood CFO estimator, it restricts the estimable CFO to less than half of the subcarrier spacing. More important, frequency-selective effects are not accounted for. A MUSIC-like method was proposed in [7] for non-data-aided CFO and channel estimation, but unfortunately, channel and CFO identifiability is not guaranteed [8]. CFO estimators exploiting the cyclic prefix are summarized in [6] for pure delay channels (see also [3] and [5] for frequency-selective channels). However, differences between using CP-based CFO estimation for frequency-selective channels and for flat fading channels were not explored in [3, 5].

In this paper, we derive non-data-aided CFO estimators for the cyclic-prefixed (CP) OFDM and for the recently proposed zero-padded (ZP) OFDM [4, 12, 14]. The system model is introduced in Section II and several schemes are derived in Section III for different OFDM systems. Performance comparisons and simulations are presented in Section IV and conclusions are drawn in Section V.

Bold upper (lower) case letters will be used for matrices (column vectors). Scalar $x_k(i)$ will denote the kth element of $\mathbf{x}(i)$. Superscript $^{\mathcal{H}}$ will stand for Hermitian, * conjugation, $\star$ convolution, † pseudo-inverse, ^{T} transpose, $\angle$ principal argument, $\otimes$ Kronecker product; $\text{diag}\{d_0, \ldots, d_{L-1}\}$ for a diagonal matrix whose diagonal is $[d_0, \ldots, d_{L-1}]$, E expectation, $\mathcal{R}$ range, and $\mathcal{N}$ null space.

II. Modeling and Problem Statement

With reference to Fig. 1 that depicts the discrete-time equivalent baseband model of a block transmission, the information stream $s(n)$ drawn randomly from a finite-alphabet is parsed into blocks: $\mathbf{s}(i) := [s(iK), s(iK+1), \ldots, s(iK+K-1)]^T$, each of length K. After a serial-to-parallel (S/P) convertion, the block $\mathbf{s}(i)$ constitutes the so-called ith OFDM symbol, that is mapped by a redundant linear transformation (matrix) $\mathcal{T}(\cdot)$, to form $\mathbf{u}(i) = \mathcal{T}(\mathbf{s}(i))$, where $\mathbf{u}(i)$ is a $P \times 1$ vector with $P > K$. Each block $\mathbf{u}(i)$ is serialized for transmission through the possibly unknown frequency-selective channel with finite impulse response (FIR) $h(l)$ of order L, that accounts not only for transmit/receive-filters $g_T(t)/g_R(t)$ and the frequency-selective multipath $g_o(t)$, but also for the timing offset τ_o that is incorporated as an unknown pure delay; i.e., with $h(t) := (g_T \star g_o \star g_R)(t)$, we define our discrete FIR equivalent channel as $h(l) := h(t-\tau_o)|_{t=lT}$, where T is the sampling period which is chosen equal to the symbol period. We select the receive-filter to have square-root Nyquist form.

The samples at the receive-filter output are (see Fig. 1):

$$x(i) = e^{j\omega_o i} \sum_{l=0}^{L} h(l)u(i-l) + w(i), \tag{1}$$

*Work in this paper was supported by the NSF Wireless Initiative grant no. 99-79443 and the ARL grant no. DAA01-98-Q-0648.

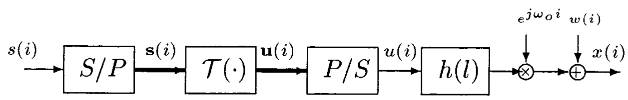

Fig. 1. Discrete-time equivalent baseband model

where: $\omega_o := 2\pi(f_c + f_{o,d})T$, f_c is the carrier frequency, $f_{o,d}$ is the CFO which is due to Doppler effects and/or mismatch between transmitter and receiver oscillators; and $w(i)$ denotes zero-mean additive white Gaussian noise (AWGN) with variance σ_w^2 that is assumed independent of the transmitted symbols.

The matrix-vector counterpart of (1) is (see e.g., [14] for a detailed derivation)

$$\mathbf{x}(i)=e^{j\omega_o iP}\mathbf{D}_P(\omega_o)[\mathbf{H}_0\mathbf{u}(i)+\mathbf{H}_1\mathbf{u}(i-1)] + \mathbf{w}(i), \qquad (2)$$

where $\mathbf{x}(i) := [x(iP), x(iP+1), \ldots, x(iP+P-1)]^T$, and likewise for $\mathbf{w}(i)$. Channel matrices $\mathbf{H}_0$ and $\mathbf{H}_1$ are $P \times P$ upper and lower triangular Toeplitz, respectively: $\mathbf{H}_0$'s first column is $[h(0), \ldots, h(L), 0, \ldots, 0]^T$ and $\mathbf{H}_1$'s first row is $[0, \ldots, 0, h(L), \ldots, h(1)]$; $\mathbf{D}_P(\omega_o)$ is a diagonal matrix: $\mathbf{D}_P(\omega_o) := \text{diag}\{1, e^{j\omega_o}, \ldots, e^{j\omega_o(P-1)}\}$.

Our goal is to obtain CFO and channel estimates based on the received blocks $\mathbf{x}(i)$ and the structure of $\mathbf{D}_P(\omega_o)$, $\mathbf{H}_0$ and $\mathbf{H}_1$. Once CFO and channel estimates are available, linear zero-forcing (ZF), minimum mean square error (MMSE), or, Decision Feedback (DFE) block equalizers can be used to recover the information block $\mathbf{s}(i)$. For uniformity and simplicity, we will test the CFO and channel estimates for symbol recovery using ZF equalization.

III. CFO and Channel Estimators

In this section, subspace-based CFO and channel estimators will be derived starting from the block transmission model (2). For the different block transmissions of this section, the mapper $\mathcal{T}(\cdot)$ assumes different forms, and separate estimators will be needed for each model.

A. Estimators for CP-OFDM

For CP-OFDM, the mapper $\mathcal{T}(\cdot)$ amounts to taking the K-point inverse FFT (IFFT) of $\mathbf{s}(i)$, and adding the CP of length $P-K$. In matrix form, these two operations yield: $\mathbf{u}(i) = \mathbf{T}_{cp}\mathbf{F}_K^{\mathcal{H}}\mathbf{s}(i)$, where $\mathbf{T}_{cp}$ is the $P \times K$ CP-inserting matrix defined as $\mathbf{T}_{cp} := [\mathbf{I}_{cp}^T, \mathbf{I}_K^T]^T$; $\mathbf{I}_K$ is the $K \times K$ identity matrix; $\mathbf{I}_{cp}$ is formed by the last $P-K$ rows of $\mathbf{I}_K$; and $\mathbf{F}_K^{\mathcal{H}}$ is the $K \times K$ IFFT matrix with (m,n)st entry $\exp(j\frac{2\pi}{K}mn)/\sqrt{K}$. To avoid inter-block interference (IBI), the CP should be at least as long as channel order L (i.e., $P-K \geq L$), and it should be discarded at the receiver. With $\mathbf{u}(i) = \mathbf{T}_{cp}\mathbf{F}_K^{\mathcal{H}}\mathbf{s}(i)$, the received block is [c.f. (2)]

$$\begin{aligned}\mathbf{x}(i) &= e^{j\omega_o iP}\mathbf{D}_P(\omega_o)[\mathbf{H}_0\mathbf{T}_{cp}\mathbf{F}_K^{\mathcal{H}}\mathbf{s}(i) \\ &\quad + \mathbf{H}_1\mathbf{T}_{cp}\mathbf{F}_K^{\mathcal{H}}\mathbf{s}(i-1)] + \mathbf{w}(i). \qquad (3)\end{aligned}$$

Carrier-offset Estimation: From the definition of $\mathbf{T}_{cp}$, it follows that the first $P-K$ elements of $\mathbf{u}(i)$ coincide with the last $P-K$ elements of $\mathbf{u}(i)$. This redundancy induces correlation between the corresponding elements of $\mathbf{x}(i)$ in (3). Specifically, the correlation of the nth with the $(n+K)$th components of $\mathbf{x}(i)$ turns out to be:

$$E[x_n^*(i)x_{n+K}(i)] = \begin{cases} \sigma_s^2 e^{j\omega_o K}\sum_{l=0}^{n}|h(l)|^2 & 0 \leq n \leq L-1 \\ \sigma_s^2 e^{j\omega_o K}\sum_{l=0}^{L}|h(l)|^2 & L \leq n \leq P-K-1 \\ \sigma_s^2 e^{j\omega_o K}\sum_{l=n-(P-K-1)}^{L}|h(l)|^2 & P-K \leq n \leq P-K+L-1 \\ 0 & P-K+L \leq n \leq P-1 \end{cases} \qquad (4)$$

where $x_n(i) := x(iP+n)$, and $\sigma_s^2 := E[|s_n(i)|^2]$. From (4), we can see that the autocorrelation of the received symbols is channel dependent unlike what is reported in [6, Eq. (2)]. The sample estimate of $E[x_n^*(i)x_{n+K}(i)]$ is given by $M^{-1}\sum_{m=0}^{M-1}x_n^*(m)x_{n+K}(m)$, where M is the number of blocks. We observe from (4) that when $L \leq n \leq P-K-1$, the absolute values of $E[x_n^*(i)x_{n+K}(i)]$ are equal to each other and achieve the maximum for all $n \in [0, P-1]$. This means that using these pairs of symbols, we can obtain more reliable CFO estimators than those found by using all the CP symbols. This is the difference between our method and [5] which our simulated performance results confirm as being important.

If $|\omega_o K| < \pi$, then a unique estimate $\hat{\omega}_o$ is offered by the sample estimate of $E[x_n^*(i)x_{n+K}(i)]$ as follows:

$$\hat{\omega}_o = \frac{1}{K}\angle\left[\frac{1}{P-K-L}\sum_{n=L}^{P-K-1}\left(\frac{1}{M}\sum_{m=0}^{M-1}x_n^*(m)x_{n+K}(m)\right)\right]. \qquad (5)$$

When M is large enough, Eq. (5) yields a reliable CFO estimate, and corroborates that the redundancy offered by the CP not only eliminates IBI, but also enables a non-data-aided method for CFO estimation.The performance of the CFO estimator in [6] depends on the CP length $P-K$ which must be $\geq L$ to avoid IBI. We will elaborate further on this point in the simulations.

Channel Estimation: Based on the CFO estimate in (5), we can remove those terms containing ω_o from $\mathbf{x}(i)$ in (3) to arrive at:

$$\bar{\mathbf{x}}(i) := \mathbf{H}_0\mathbf{T}_{cp}\mathbf{F}_K^{\mathcal{H}}\mathbf{s}(i) + \mathbf{H}_1\mathbf{T}_{cp}\mathbf{F}_K^{\mathcal{H}}\mathbf{s}(i-1) + \bar{\mathbf{w}}(i), \qquad (6)$$

where $\bar{\mathbf{w}}(i) := e^{-j\omega_o iP}\mathbf{D}_P^{\mathcal{H}}(\omega_o)\mathbf{w}(i)$. Next, we discard the CP-induced redundancy by forming $\mathbf{R}_{cp}\bar{\mathbf{x}}(i) := [\mathbf{0}_{K\times(P-K)}, \mathbf{I}_K]\bar{\mathbf{x}}(i)$, which cancels IBI at the receiver since $\mathbf{R}_{cp}\mathbf{H}_1 = \mathbf{0}$. It can be verified that $\mathbf{R}_{cp}\mathbf{H}_0\mathbf{T}_{cp} = \tilde{\mathbf{H}}$, where the $K \times K$ matrix $\tilde{\mathbf{H}}$ is circulant with first row $[h(0), 0, \ldots, 0, h(L), \ldots, h(1)]$. Recalling that for a circulant $\tilde{\mathbf{H}}$, the matrix $\mathbf{F}_K\tilde{\mathbf{H}}\mathbf{F}_K^{\mathcal{H}}$ is diagonal, one can FFT process the IBI-free blocks, to obtain

$$\begin{aligned}\mathbf{y}(i) &:= \mathbf{F}_K\mathbf{R}_{cp}\bar{\mathbf{x}}(i) = \mathbf{F}_K\mathbf{R}_{cp}\mathbf{H}_0\mathbf{T}_{cp}\mathbf{F}_K^{\mathcal{H}}\mathbf{s}(i) + \mathbf{v}(i) \\ &= \mathbf{D}_K(\mathrm{H})\mathbf{s}(i) + \mathbf{v}(i), \qquad (7)\end{aligned}$$

where $\mathbf{v}(i) := \mathbf{F}_K\mathbf{R}_{cp}\bar{\mathbf{w}}(i)$, and $\mathbf{F}_K\tilde{\mathbf{H}}\mathbf{F}_K^{\mathcal{H}} = \mathbf{D}_K(\mathrm{H}) := \text{diag}\{H(0), \ldots, H(2\pi(K-1)/K)\}$, with $H(2\pi k/K) :=$

$\sum_{l=0}^{L} h(l)\exp(-j2\pi lk/K)$, $k = 0, 1, \ldots, K-1$. Eq. (7) confirms that after removing the CFO and IBI, FFT processing converts the frequency-selective channel (described by the convolution matrices $\mathbf{H}_0, \mathbf{H}_1$ in (3)) to a set of flat-fading subchannels that appear on the diagonal entries of $\mathbf{D}_K(\mathrm{H})$ in (7).

Estimation of the channel's frequency response on the FFT grid can be performed based on training symbols $\check{\mathbf{s}}(i)$. Specifically, letting $\tilde{\mathbf{h}} := [H(0), \ldots, H(2\pi(K-1)/K)]^T$, one can rewrite $\mathbf{D}_K(\mathrm{H})\check{\mathbf{s}}(i) = \mathbf{D}_K(\check{\mathbf{s}}(i))\tilde{\mathbf{h}}$, and solve (7) for $\tilde{\mathbf{h}}$ in the least-squares sense.

Blind and semi-blind algorithms for channel estimation and tracking are also possible and are well motivated when the channel variations are rapid and frequent retraining consumes considerable bandwidth. Particularly appealing for our non-data-aided context are the (semi-)blind approaches in [15] that rely on the blocks $\mathbf{y}(i)$ of (7) and exploit the finite alphabet of $\mathbf{s}(i)$ to come up with a low-complexity/high-performance channel estimation algorithm that was tested successfully on realistic HIPERLAN/2 settings.

B. Estimators for ZP-OFDM

The difference between ZP-OFDM and CP-OFDM transmissions is that the redundant cyclic prefix is replaced by zero-padding. Instead of $\mathbf{T}_{cp}$, the transmit matrix now is $\mathbf{T}_{zp} := [\mathbf{I}_K^T, \mathbf{0}_{(P-K)\times K}^T]^T$. Since ZP-OFDM does not rely on the replicated symbols that we exploited in Section III.A for CFO estimation, here we will first target channel estimation based on a subspace approach and then estimate the CFO. The channel estimator for ZP-OFDM is also discussed in [2, 12], but here we consider CFO estimation as well.

In the presence of CFO and frequency-selective multipath, the received block in ZP-OFDM is:

$$\mathbf{x}(i) = e^{j\omega_o iP}\mathbf{D}_P(\omega_o)\mathbf{H}_0\mathbf{T}_{zp}\mathbf{F}_K^{\mathcal{H}}\mathbf{s}(i) + \mathbf{w}(i), \qquad (8)$$

where IBI has been eliminated from (2) because $\mathbf{u}(i) = \mathbf{T}_{zp}\mathbf{F}_K^{\mathcal{H}}\mathbf{s}(i)$ and $\mathbf{H}_1\mathbf{T}_{zp} = \mathbf{0}$. By observing that $\mathbf{H}_0$ is lower triangular and $\mathbf{D}_P(\omega_o)$ is diagonal, one can verify that $\mathbf{D}_P(\omega_o)\mathbf{H}_0 = \bar{\mathbf{H}}_0\mathbf{D}_P(\omega_o)$, where $\bar{\mathbf{H}}_0$ is what we term *auxiliary channel*, which has the same structure as $\mathbf{H}_0$ but with entries $\bar{h}(l) := e^{j\omega_o l}h(l), l = 0, 1, \ldots, L$. It can be verified by direct substitution that $\mathbf{D}_P(\omega_o)\mathbf{T}_{zp} = \mathbf{T}_{zp}\mathbf{D}_K(\omega_o)$, where $\mathbf{D}_K(\omega_o) := \mathrm{diag}\{1, e^{j\omega_o}, \ldots, e^{j\omega_o(K-1)}\}$. Letting $\bar{\mathbf{H}}_0 := [\bar{\mathbf{H}}, \bar{\mathbf{H}}_{zp}]$, with $\bar{\mathbf{H}}$ and $\bar{\mathbf{H}}_{zp}$ representing the first K and last $P-K$ columns of $\bar{\mathbf{H}}_0$, respectively, the received block can be rewritten as [c.f. (8)]

$$\mathbf{x}(i) = e^{j\omega_o iP}\bar{\mathbf{H}}\mathbf{D}_K(\omega_o)\mathbf{F}_K^{\mathcal{H}}\mathbf{s}(i) + \mathbf{w}(i). \qquad (9)$$

Based on (9), we will derive estimators for the auxiliary channel $\bar{h}(l)$ and the CFO ω_o.

Channel Estimation: Suppose that we select:
a1) the transmitted block size $P = K + L$.

Noting that $\bar{\mathbf{H}}$ in (9) is a tall matrix, prompts us to pursue low-rank decompositions of data matrices and subspace methods for channel estimation. Upon defining the matrices $\mathbf{D}_o := \mathrm{diag}\{1, e^{j\omega_o P}, \ldots, e^{j\omega_o(M-1)P}\}$, $\mathbf{X} := [\mathbf{x}(0), \ldots, \mathbf{x}(M-1)]$, and likewise for $\mathbf{S}$ and $\mathbf{W}$, we find

$$\mathbf{X} = \bar{\mathbf{H}}\mathbf{D}_K(\omega_o)\mathbf{F}_K^{\mathcal{H}}\mathbf{S}\mathbf{D}_o + \mathbf{W}, \qquad (10)$$

which in the noiseless case leads to

$$\mathbf{X}\mathbf{X}^{\mathcal{H}} = \bar{\mathbf{H}}\mathbf{D}_K(\omega_o)\mathbf{F}_K^{\mathcal{H}}\mathbf{S}\mathbf{D}_o\mathbf{D}_o^{\mathcal{H}}\mathbf{S}^{\mathcal{H}}\mathbf{F}_K\mathbf{D}_K^{\mathcal{H}}(\omega_o)\bar{\mathbf{H}}^{\mathcal{H}}. \qquad (11)$$

We also collect a sufficient number of received blocks M to assure that:
a2) M is large enough so that $\mathbf{S}\mathbf{S}^{\mathcal{H}}$ has full rank K.
Under a1), a2), and the fact that matrices $\mathbf{D}_K(\omega_o)$, $\mathbf{F}_K$ and $\bar{\mathbf{H}}$ have full column rank K, we infer that rank $(\mathbf{X}\mathbf{X}^{\mathcal{H}}) = K$, and that $\mathcal{N}(\mathbf{X}\mathbf{X}^{\mathcal{H}}) = \mathcal{N}(\bar{\mathbf{H}})$.

By eigen-decomposing $\mathbf{X}\mathbf{X}^{\mathcal{H}}$, we thus obtain

$$\mathbf{X}\mathbf{X}^{\mathcal{H}} = [\mathbf{U}, \tilde{\mathbf{U}}]\begin{bmatrix}\mathbf{\Sigma}_{K\times K} & \mathbf{0}_{K\times(P-K)} \\ \mathbf{0}_{(P-K)\times K} & \mathbf{0}_{(P-K)\times(P-K)}\end{bmatrix}\begin{bmatrix}\mathbf{U}^{\mathcal{H}} \\ \tilde{\mathbf{U}}^{\mathcal{H}}\end{bmatrix}. \qquad (12)$$

The columns of $\tilde{\mathbf{U}}$ span $\mathcal{N}(\bar{\mathbf{H}})$; hence, the lth column of $\tilde{\mathbf{U}}$ satisfies $\tilde{\mathbf{u}}_l^{\mathcal{H}}\bar{\mathbf{H}} = \mathbf{0}^{\mathcal{H}}$, for $l = 1, \ldots, P-K$. Since $\bar{\mathbf{H}}$ is Toeplitz, the commutativity of convolution implies that

$$\tilde{\mathbf{u}}_l^{\mathcal{H}}\bar{\mathbf{H}} = \bar{\mathbf{h}}^T\tilde{\mathbf{U}}_l, \qquad l = 1, \ldots, P-K, \qquad (13)$$

where $\bar{\mathbf{h}} := [\bar{h}(0), \ldots, \bar{h}(L)]^T$, and $\tilde{\mathbf{U}}_l$ is a Hankel matrix formed by $\tilde{\mathbf{u}}_l$ as follows ($u_l(m)$ is the mth entry of $\tilde{\mathbf{u}}_l$):

$$\tilde{\mathbf{U}}_l = \begin{bmatrix} u_l^*(1) & u_l^*(2) & \cdots & u_l^*(K) \\ u_l^*(2) & u_l^*(3) & \cdots & u_l^*(K+1) \\ \vdots & \vdots & \vdots & \vdots \\ u_l^*(L+1) & u_l^*(L+2) & \cdots & u_l^*(K+L) \end{bmatrix}. \qquad (14)$$

Stacking all the equations from (13), we obtain

$$\bar{\mathbf{h}}^T\tilde{\mathbf{U}} := \bar{\mathbf{h}}^T[\tilde{\mathbf{U}}_1, \tilde{\mathbf{U}}_2, \ldots, \tilde{\mathbf{U}}_{P-K}] = \mathbf{0}_{1\times K(P-K)}^T, \qquad (15)$$

which can be solved uniquely to yield $\bar{\mathbf{h}}$ within a scalar (that is inherently present in all blind methods) as the null eigenvector of $\tilde{\mathbf{U}}$ in (15) [2, 12]. In the presence of noise, $\bar{\mathbf{h}}$ is estimated as the unique eigenvector in (15) corresponding to the minimum eigenvalue.

Performance analysis for this channel estimator was given in [2]. The capability of the estimator in (15) to cope with CFO relies on two important points: i) $\mathbf{D}_K(\omega_o)$ and $\mathbf{F}_K$ are full rank; and ii) $\mathbf{D}_P(\omega_o)$ and $\mathbf{T}_{zp}$ are interchangeable. Based on i) and ii) we can estimate and equalize the auxiliary channel first and subsequently take care of the CFO (in contrast with CP-OFDM that estimates the CFO first). Since a method to estimate and compensate for the CFO so that symbol recovery can be achieved was not given in [2, 12], we derive such a blind estimator for CFO next.

Carrier-offset Estimation: Having identified $\bar{\mathbf{H}}$, we

0-7803-7097-1/01/$10.00 ©2001 IEEE

have several possibilities to equalize the channel from the received data. Define the $K \times 1$ vector $\mathbf{y}(i) := \mathbf{G}\mathbf{x}(i)$, where $\mathbf{G} = \bar{\mathbf{H}}^{\dagger}$ for the ZF equalizer option, and $\mathbf{G} = \mathbf{R}_{ss}\bar{\mathbf{H}}^{\mathcal{H}}(\sigma_w^2\mathbf{I}+\bar{\mathbf{H}}\mathbf{R}_{ss}\bar{\mathbf{H}}^{\mathcal{H}})^{-1}$ for the MMSE. Supposing perfect channel knowledge, the equalizer $\mathbf{G}$ removes the auxiliary channel but colors the noise in (9) as $\mathbf{n}(i) := \mathbf{G}\mathbf{w}(i)$ to yield:

$$\mathbf{y}(i) := \mathbf{G}\mathbf{x}(i) = e^{j\omega_o iP}\mathbf{D}_K(\omega_o)\mathbf{F}_K^{\mathcal{H}}\mathbf{s}(i) + \mathbf{n}(i). \quad (16)$$

Given $\{\mathbf{y}(i), \check{\mathbf{s}}(i)\}_{i=1}^{I}$, data-aided CFO approaches are readily applicable and consist of solving (16) for ω_o. However, blind CFO estimators are also possible by using the transmitted signal's finite-alphabet. When the transmitted signal adheres to a finite-alphabet constellation, say PSK, there exists an integer J so that $s^J(n) = \alpha_s$, which is a constant. For BPSK, we have $J = 2$, $s_k^2(i) = \mathcal{E}_s$, and for QPSK and QAM, $J = 4$, $s_k^4(i) = -\mathcal{E}_s^2$, where $\mathcal{E}_s$ is the symbol energy.

Now our goal is to estimate ω_o from $\mathbf{y}(i)$. Define $\bar{\mathbf{y}}(i,\omega) = \exp(-j\omega iP)\mathbf{F}_K\mathbf{D}_K^{\mathcal{H}}(\omega)\mathbf{y}(i)$, where denotes ω is the candidate CFO. In the absence of noise, if $\omega = \omega_o$, one can verify that $\bar{\mathbf{y}}(i,\omega) = \mathbf{s}(i)$; i.e., $\bar{y}_m^J(i,\omega) = \alpha_s$. Thus, a CFO estimator can be obtained as:

$$\hat{\omega}_o = \arg\min_{\omega} \sum_{i=0}^{N_b-1}\sum_{m=0}^{K-1} |\bar{y}_m^J(i,\omega) - \alpha_s|^2. \quad (17)$$

Adaptive algorithms (e.g., LMS, RLS) can be considered here to find the minimum. Simulations indicate that reliable CFO estimates can be obtained from (17).

Comparing Section III.A with III.B, one recognizes two main differences: i) In Section III.A, we estimate the CFO first and identify the channel afterwards, but in Section III.B, the order is reversed; ii) For CP-OFDM, the estimates rely on statistical averages, while for ZP-OFDM, deterministic methods are employed. One of the advantages of deterministic methods is their data efficiency. A natural question arises on the preferred order which estimation for CFO and channel should be performed. Simulations suggest that estimators for ZP-OFDM outperform those for CP-OFDM.

IV. Simulated Performance

We have outlined so far two basic approaches for blind CFO and channel estimation in single-user multicarrier transmissions. In the following, we will present examples to illustrate the performance of these schemes and compare them with [6]. In our simulations, the noise $w(i)$ in (1) is zero mean AWGN with variance σ_w^2. For all examples, QPSK modulation is employed. The frequency-selective channel taps are generated independently as complex Gaussian variables (Rayleigh channels). The definition of signal to noise ratio (SNR) used in these examples is: $SNR := \mathcal{E}_s/\sigma_w^2$, with normalized channel variance; i.e., $\sigma_h^2 = 1$, where $\mathcal{E}_s$ is the energy per symbol.

Example 1: `(CP-OFDM with CFO)` Here we will assess the performance of the proposed estimators for CP-OFDM. We choose FFT size $K = 16$ and test the effects of the CP length $N - K$ and the channel order L on performance. The normalized CFO ω_o is chosen to be random uniformly distributed on $[-\pi/K, \pi/K]$. The bit-error-rate (BER) and mean square error (MSE) of the CFO are averaged over $1,800$ randomly generated channels and CFO values. For each channel and CFO realization, we use 100 blocks of received data. From Fig. 2, we observe that for fixed channel order L, the longer the CP is, the better performance we obtain. For a fixed CP length, we can verify that performance improves as the channel order decreases. The MSE of channel estimates is similar to that in [15]. In the same figure, we compare our method with the minimum variance unbiased (MVU) estimator in [6]. Fig. 2 verifies that our estimator outperforms [6].

Example 2: `(ZP-OFDM with CFO)` This example tests the performance of the estimators proposed in Section III.B. Similar to Example 1, we choose parameters $K = 16$, $N = 24$ and $L = 4$. The BER and MSE of CFO are averaged over $1,000$ channel realizations with 40 blocks of data used per realization. From the discussion in Section III.A, we know that the subcarrier ambiguity problem limits the correctable CFO range within $[-\pi/K, \pi/K]$ for CP-OFDM. However, for ZP-OFDM, we do not have this problem. The correctable CFO range can be extended to $[-\pi, \pi]$. For fairness, in Fig. 3, the normalized CFO ω_o is chosen to be uniformly distributed in $[-\pi/K, \pi/K]$. In order to benchmark the performance of our CFO and channel estimators, we plotted the BER when the channel and CFO are perfectly known in Fig. 3. It can be seen that the proposed method has good performance. From Fig. 3, we can also see that MMSE equalizer gains about 4.5 dB for a BER of 10^{-2}.

Comparing Fig. 2 with Fig. 3, we observe that ZP-OFDM outperforms CP-OFDM even with less blocks of data because the former relies on a deterministic (subspace) channel estimator and exhaustive search for CFO estimation, while the latter depends on statistical averages. The following example will further illuminate this point.

Example 3: `(ZP-OFDM vs. CP-OFDM)` In this example, we will compare ZP-OFDM with CP-OFDM using fixed channels and CFOs. The channel taps are given as $\mathbf{h} = [-0.1222 + 0.05257i, 0.3049 + 0.4229i, 0.0489 + 0.1252i, 0.3605-0.2729i, -0.5169+0.4698i]^T$, and the CFO $\omega_o = 0.01\pi$. The system parameters are $[P, K, L] = [24, 16, 4]$. From Fig. 4, we observe that ZP-OFDM outperforms CP-OFDM considerably. For ZP-OFDM, we can see that linear MMSE equalization exhibits better performance than linear ZF at low SNR. We plotted CRBs of CFOs as benchmarks to evaluate our proposed methods. From Fig. 4 (right), we can see that the CFO MSE of

ZP-OFDM converges to the CRB faster than CP-OFDM. Note that in Fig. 4, the CRB of the CFO estimator for CP-OFDM is lower than that for ZP-OFDM. The main reason here is that the ZP part reduces power requirements relative to CP.

V. Conclusions and Research Directions

In this paper, we proposed several carrier frequency offset and channel (that also includes timing) estimation schemes for OFDM systems. Although emphasis was placed on single-user point-to-point links, our algorithms are also directly applicable to multiuser multicarrier schemes (such as MC-CDMA) in the *downlink*, where each user receives the superimposed transmissions through its own (but yet a single) CFO and frequency-selective channel. The features of the proposed methods are:

i) they are blind, and hence they do not consume extra bandwidth that comes with frequent retraining;

ii) they guarantee uniqueness of CFO and channel estimates.

For CP-OFDM, we developed a statistical CFO estimator. Comparing CP- with ZP-OFDM, the latter exhibits better performance. Current research efforts focus on deterministic blind approaches for CFO estimation in CP-OFDM. The subject deserving further investigation is extending the present estimators to multi-carrier multi-user systems, in the *uplink*, where multiple user-specific CFOs and channels need to be accounted for. Preliminary results in this direction deal with timing and carrier synchronization of the generalized OFDMA scheme in [14], which has performance invariant to channel nulls [1].

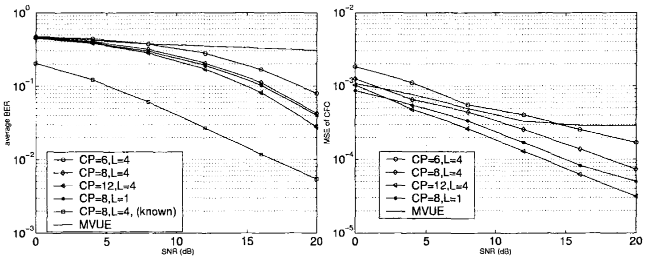

Fig. 2. BER (left) and MSE (right) vs. E_s/N_0 for CP-OFDM

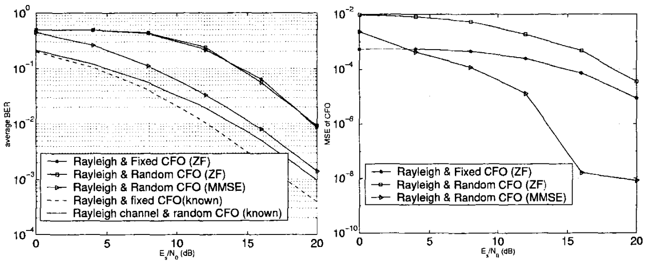

Fig. 3. BER (left) and MSE (right) vs. E_s/N_0 for ZP-OFDM

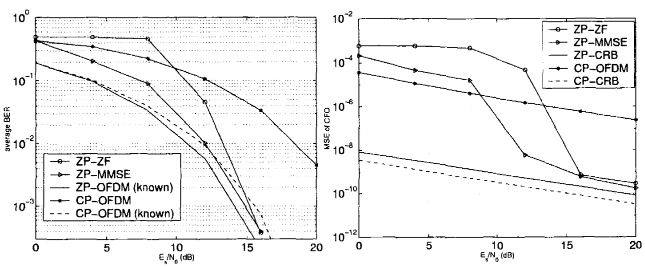

Fig. 4. Comparisons between ZP-OFDM and CP-OFDM

References

[1] S. Barbarossa, M. Pompili and G. B. Giannakis, "Time and Frequency Syncronization of Orthogonal Frequency Division Multiple Access Systems," *Proc. of Inter. Conf. on Comm.*, Helsinki, Finland, 2001.

[2] S. Barbarossa, A. Scaglione and G. B. Giannakis, "Performance Analysis of a Deterministic Channel Estimation for Block Transmission Systems with Null Guard Intervals," *IEEE Trans. on Signal Processing*, 2001.

[3] J. van de Beek, M. Sandell and P. O. Börjesson, "ML Estimation of Time and Frequency Offset in OFDM Systems," *IEEE Trans. on Signal Processing*, vol. 45, pp. 1800–1805, July 1997.

[4] G. B. Giannakis, "Filterbanks for Blind Channel Identification and Equalization," *IEEE Signal Processing Letters*, vol. 4, pp. 184–186, June 1997.

[5] M. H. Hsieh, C. H. Wei, "A Low-Complexity Frame Synchronization and Frequency Offset Compensation Scheme for OFDM Systems over Fading Channels," *IEEE Trans. on Veh. Tech.*, vol. 48, pp. 1596–1609, Sep. 1999.

[6] N. Lashkarian and S. Kiaei, "Class of Cyclic-Based Estimators for Frequency-Offset Estimation of OFDM Systems," *IEEE Trans. on Comm.*, vol. 48, pp. 2139–2149, Dec. 2000.

[7] H. Liu and U. Tureli, "A High-Efficiency Carrier Estimator for OFDM Communications," *IEEE Comm. Letters*, vol. 2, pp. 104–106, Apr. 1998.

[8] X. Ma, C. Tepedelenlioğlu and G. B. Giannakis, "Consistent Blind Synchronization of OFDM Transmissions Using Null Sub-Carriers with Distinct Spacings," *Proc. of IEEE SPAWC*, Taiwan, R.O.C., March 20-23, 2001.

[9] P. H. Moose, "A Technique for Orthogonal Frequency Division Multiplexing Frequency Offset Correction," *IEEE Trans. on Comm.*, vol. 42, no. 10, Oct. 1994.

[10] M. Morelli and U. Mengali, "An Improved Frequency Offset Estimator for OFDM Applications," *IEEE Comm. Letters*, vol. 3, no. 3, pp. 75–77, Mar. 1999.

[11] T. Pollet, M. V. Bladel and M. Moeneclaey, "BER Sensitivity of OFDM Systems to Carrier Frequency Offset and Wiener Phase Noise," *IEEE Trans. on Comm.*, vol. 43, pp. 191–193, Feb./Mar./Apr. 1995.

[12] A. Scaglione, G. B. Giannakis and S. Barbarossa, "Redundant Filterbank Precoders and Equalizers Part II: Blind Channel Estimation, Synchronization and Direct Equalization," *IEEE Trans. on Signal Processing*, vol. 47, pp. 1988–2022, July 1999.

[13] T. M. Schmidl and D. C. Cox, "Robust Frequency and Timing Synchronization for OFDM," *IEEE Trans. on Comm.*, vol. 45, no. 12, pp. 1613–1621, Dec. 1997.

[14] Z. Wang and G. B. Giannakis, "Wireless Multicarrier Communications: where Fourier meets Shannon," *IEEE Signal Processing Magazine*, vol. 17, no. 3, pp. 29–48, May 2000.

[15] S. Zhou and G. B. Giannakis, "Finite-Alphabet Based Channel Estimation for OFDM and related Multi-Carrier Systems," *IEEE Trans. on Comm.*, 2001.